

# MORPHOLOGICAL TUBULAR EXTRACTION APPLIED TO CORONARY ARTERY RECONSTRUCTION IN CT-IMAGES

M.A. Luengo-Oroz<sup>§</sup>, M.J. Ledesma-Carbayo<sup>§</sup>, J.J. Gómez-Diego<sup>‡</sup>, M.A. García-Fernández<sup>‡</sup>, M.Desco<sup>‡</sup> and A. Santos<sup>§</sup>

<sup>§</sup>Biomedical Image Technologies lab., ETSIT, Universidad Politécnica de Madrid, Av. Complutense S/N, Madrid, Spain

<sup>‡</sup>Hospital General Universitario Gregorio Marañón, C/ Doctor Esquerdo 46, Madrid, Spain

maluengo@die.upm.es, mledesma@die.upm.es, josejgd@telefonica.net,

magfeco@primus.es, desco@mce.hggm.es, andres@die.upm.es

## ABSTRACT

This paper presents an algorithm devoted to the reconstruction of the coronary tree from Cardiac Multislice CT data sets. Quantitative measurement of this segmentation may help the diagnosis and treatment of ischemic heart disease. The algorithm is based on morphological grayscale reconstruction through 2D slice images and overall 3D segmentation of the coronary artery tree. The method has been validated in 9 CT-datasets with satisfactory results.

## KEY WORDS

coronary tree, multi-slice computer tomography, segmentation, mathematical morphology.

## 1 Introduction

Cardiovascular disease is the leading cause of death in many countries. The conventional way of imaging coronary arteries is by using invasive coronary angiography, but this technique brings complicated clinical procedures and risks to the patient. Recent technical developments have converted CT in a very interesting alternative for imaging coronary arteries. CT imaging is a non-invasive imaging technique, that provides information of the whole 3D volumetric data with high resolution. An intravenous contrast agent is used to enhance the visibility of blood, and consequently the vessels. The areas containing the contrast agent are marked in the resultant output images with a larger Hounsfield value. Therefore, the segmentation of the coronary arteries provides a valuable diagnostic tool for clinicians interested in detecting plaques, calcifications or stenosis. However, segmentation of the coronary tree is a difficult task due to low contrast conditions, the vicinity to the heart cavities, and its complex structure, including branching and curvatures. Furthermore, for real applications a fast and efficient approach is desired. From a medical imaging point of view, vessel segmentation (there is a very complete review in [8]) is the core of many medical applications such as diagnosis systems, image registration, visualization or computer-guided surgery. However segmentation is still an open problem with many methods depending on the imaging modality, the human interaction and many other factors. Concerning recent publications on segmentation of the CT cardiac tree, we find

several promising attempts in early stages of development such as [13], based on active contour models. In [9], the segmentation is achieved using a combination of thresholding, region-growing, and morphological operations. Indeed, a very good visualization interface is provided, however the segmentation algorithm gives false positives. In [6], a particle-based approach to vessel segmentation is performed with interesting results, but non principal branches are missed. Regarding general problems with other segmentations methods, we find that level-sets are not suited for real-time applications because they are computational time-consuming; parametric cylindrical models may not be suited for the non-linearity of vessel structures and region-growing techniques may be sensitive to local conditions. Because of these difficulties on the accurate detection of the whole coronary tree, we propose a prior robust and fast segmentation technique based on mathematical morphology that extracts the entire coronary tree from an initial click given by the human expert. In this reconstruction our goal is not to lose any information even in pathological cases. In a second stage, the coronary tree would be segmented into different regions such as lumen, plaque or calcium; in order to give quantitative measurements to help the diagnosis of calcifications and stenosis. This article is going to lead with the first phase of the proposed approach and it is organized as follows: firstly, we present the MACTSE algorithm used for the coronary tree reconstruction. Then we present and discuss the segmentation in 9 clinical data sets. Finally we discuss the results and further developments.

## 2 Morphological algorithm for causal tubular structures extraction (MACTSE)

### 2.1 Theoretical framework

Mathematical morphology is a powerful nonlinear image technique with operators capable of handling sophisticated image processing tasks in binary, grey-scale, colour and multiresolution imaging modalities based on geometric analysis. A tutorial on the technique can be found in [11]. These techniques have been widely used in vessel extraction with successful results [14] and also in segmentation and quantification of 2D angiograms [2, 10]. Morphological grayscale reconstruction methods through

2D slice images and overall 3D reconstruction has been previously used in [7] for the segmentation of the airway tree with successful results. In the case of the coronary artery tree, the image conditions are different as there are not as many scale changes in the coronary arteries as in bronchia and the existence of other surrounding structures may difficult the segmentation process. This contextual information has been used to develop a specific algorithm.

The basic morphological operators are dilation  $\delta_B(f(x)) = \sup_{y \in B} \{f(x - y)\}$  and erosion  $\varepsilon_B(f(x)) = \inf_{-y \in B} \{f(x - y)\}$ . These two elementary operations can be composed together to yield a new set of operators having desirable feature extractor properties which are given by opening  $\gamma_B(f) = \delta_B[\varepsilon_B(f)]$  and closing  $\varphi_B(f) = \varepsilon_B[\delta_B(f)]$ . Morphological *openings* (*closings*) filter out light (dark) structures from the images according to the predefined size and shape criterion of the structuring element. The main morphological operator we use is the morphological reconstruction by dilation [12] which consists in reconstructing a mask image from a marker image by iterating geodesic dilations of the marker image inside the mask image until stability (see fig. 3). We denote by  $f$  the marker image and by  $g$  the mask image. The geodesic dilation with structuring element  $B$  of the marker image  $f$  with respect to the mask image  $g$  is  $\delta_g^n(f) = \delta_g^1 \delta_g^{n-1}(f)$ , where  $\delta_B^1(f, g) = \delta_B(f) \wedge g$ ;  $\delta_B^1(f)$  indicates a dilation of image  $f$  by the structuring element  $B$  restricted to  $g$ . The reconstruction by dilation of mask  $g$  from marker  $f$ , is denoted  $R_B(f, g) = \delta_B^i(f, g)$  where  $i$  is chosen such that  $\delta_B^i(f, g) = \delta_B^{i+1}(f, g)$  (idempotence).

## 2.2 General architecture

The general structure of the algorithm is the following (see fig.1):

- 1) The human expert selects a point as a marker in the first slice where it is found the coronary artery. We use the hypothesis that the artery is a causal structure along the z-axis (there is no possibility for the artery to grow backwards)
- 2) The proposed segmentation method is performed from the mark in the 2D slice  $i$ .
- 3) The human expert selection is automatically generated in the slice  $i+1$ . A set of potential marks is automatically provided for the morphological segmentation of the slice  $i+1$ .
- 4) The process of segmentation is performed again in the slice  $i+1$ , which generates a set of potential marks for the slice  $i+2$ . These steps are iterated until there is no set of potential marks for the prolongation of the tubular structure.

It is important to remark that the output is not a binary segmentation but a grey-level reconstruction of the ROI with levels of intensity in each slice corresponding to the difference from the vessel to the background (the plate zone around the vessel). Pre-knowledge from the charac-

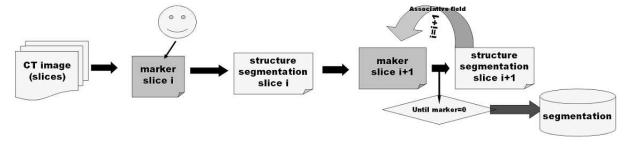


Figure 1. Scheme of the architecture of MACTSE.

teristics of the tubular structures provides us two key features for the segmentation algorithm:

- a) Inspired by the principle of *good-continuation* from psychological Gestalt's theory and its interpretation in terms of human vision [5], we use the notion of *associative field*. Let  $T$  be a tubular causal structure along the z-axis. We define the *associative field* from the cross-section of  $T$  in the slice  $i$  (XY plan) as the 2D region in slice  $i + 1$  where there is high probability to find a cross-section of the previous tubular structure(see fig.2).
- b) As it has been studied in generalized cylinders models [1], the cross-section function of a tube is defined by an ellipse (a circle when the spine of the tube corresponds with the z-axis). Even in the case of bifurcation we could have several ellipses. In MACTSE, we use the fact that all the connected regions of a cross-section from the tubular structure have at least one direction that measures the same as the diameter of the real tube(see fig.2).

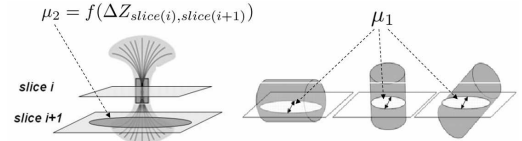


Figure 2. Parameters  $\mu_2$  and  $\mu_1$  are function of the associative field and the maximum diameter allowed to a vessel.

## 2.3 Implementation details

The MACTSE works as follows. Let  $(S_i)$  be the first image where it is possible to find a coronary artery,  $(M_i)$  the mark selected by the human expert and  $B_i$  is a disc structuring element of size  $i$ .

- 1)  $(IR_i) = R_{B_i}(M_i, S_i)$
- 2)  $(SG_i) = IR_i - R_{B_i}(\gamma_{B_{\mu_1}}(IR_i), IR_i)$
- 3)  $(MS_i) = Threshold_\lambda(SG_i)$
- 4)  $(A_i) = \delta_{B_{\mu_2}}(MS_i)$
- 5)  $(B(i+1)) = (S(i+1)) \wedge (A_i)$
- 6)  $(M(i+1)) = RegionalMaxima(B(i+1))$
- 7) If  $(M(i+1)) = 0$  then [end]  
else [step1( $M(i+1)$ ,  $S(i+1)$ )]

Steps 1,2 are devoted to the one-slice segmentation (see fig. 3). First by highlighting the marked regions with the reconstruction by dilation of the original image. Then the top-hat opening by reconstruction is used to extract only the light tubular-like structures. As a z-section of these arteries has at least one direction with a measure similar to the artery diameter, this diameter is a minimum for the size of the structuring element  $B_{\mu_1}$ . So the parameter  $\mu_1$  is directly correlated to the diameter of the searched tubular structure.

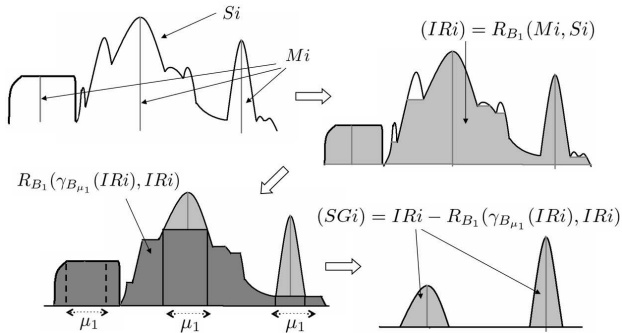


Figure 3. Schema of the segmentation of the vessel candidates in one slice.

From step 3 to step 7, the associative field for the slice  $S(i+1)$  is created by the dilation of the binary mask of the segmentation of the slice  $S_i$ . The marks that are used for the segmentation of  $S(i+1)$  are all the regional maxima from the intersection of the associative field and the original slice. We suppose that these regional maxima are a good approximation of the hypothetic selection of a human expert. This process is iterated until there are no marks for the next slice segmentation. It is worth noting the fact that the parameter  $\mu_2$  is directly related to the size of the associative field considered. Furthermore, the size of this associative field should be adjusted in function of the distance between two slices so  $\mu_2 = f(\Delta Z_{slice(i), slice(i+1)})$ . This parameter allows tracking the tubular structure even in undersampled z-axis images where the continuation of the tube is not so closely aligned in two consecutive slices. Generally, the segmentation results may be mathematically described in function of the parameters regarding the property of ordering preservation of morphological operators ( $X \leq Y \Rightarrow \Psi(X) \leq \Psi(Y)$ ). Let  $S(\mu_1, \mu_2, \lambda, I)$  be the segmentation of the image  $(I)$ . So  $\mu_{1a} \leq \mu_{1b} \Rightarrow S(\mu_{1a}, \mu_2, \lambda, I) \leq S(\mu_{1b}, \mu_2, \lambda, I)$ ; and  $\mu_{2a} \leq \mu_{2b} \Rightarrow S(\mu_1, \mu_{2a}, \lambda, I) \leq S(\mu_1, \mu_{2b}, \lambda, I)$ ; and  $\lambda_a \leq \lambda_b \Rightarrow S(\mu_1, \mu_2, \lambda_a, I) \geq S(\mu_1, \mu_2, \lambda_b, I)$ . These order relationships allow to construct a hierarchy of embedded segmentations with increasing details by modifying  $\mu_1 \uparrow, \mu_2 \uparrow$  or  $\lambda \downarrow$ .

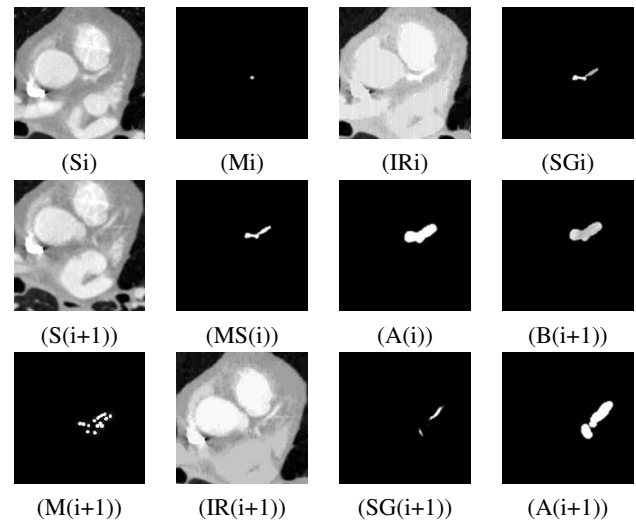


Figure 4. MACTSE procedure example.

### 3 Coronary artery segmentation from CT-images

#### 3.1 Data analyzed

The reconstruction algorithm has been tested on 9 3D-CT data sets. The images were acquired with a Toshiba Aquilion 16 CT scanner with a slice resolution of  $0.5mm$  and a slice spacing of  $0.5mm$  (isotropic). Five of the cases present minimal or inexistent lesions. The other four cases present medium or severe problems. The original data has a size of  $512 \times 512$  in the horizontal plane and between 200 and 300 slices for the z-axis. No pre-processing has been done in the images. The number and length of visible coronary artery segments differs largely in the set of patient data particularly in pathological cases. We restricted the analysis to the left coronary arteries: the left anterior descending (LAD) coronary artery and the left circumflex (LCX) coronary artery and their branches. The segmentation results have been visually evaluated by an expert.

#### 3.2 Reconstruction results and discussion

The proposed algorithm has reconstructed the entire left coronary tree in most of the normal and pathological cases (see table 1 and fig. 5). In order to achieve the best reconstruction, the parameters have been manually tuned in each case. The optimal three parameter choice vary in the following subsets:  $\mu_1 \in \{8, 9, 10\}$ ,  $\mu_2 \in \{2, 3, 4\}$ ,  $\lambda \in \{1, 2, 3\}$ . A choice of  $\mu_1 = 8, \mu_2 = 3, \lambda = 3$  provides acceptable results detecting the main branchings in 5 of the cases. However the small range of variability of the parameters could be interesting for the implementation of a user interaction interface. The main drawback of the algorithm is the extraction in most of the cases of false positives in the lowest half of the vessel tree (we can argue that

Patient	(i)	(ii)	(iii)	(iv)	(v)
a	1	3	Yes	V	4
b	1	1	Yes	$W(\frac{3}{4})$	1
c	1	4	Yes	V	3
d	2	4	Yes	No	2
e	2	4	Yes	$W(\frac{2}{3})$	3
f	3,stent	2	NO LAD	No	1
g	4	3	Yes	No	3
h	4	3	Yes	$W(\frac{1}{2})$	3
i	4,stent	3	Yes	$W(\frac{3}{4})$	3

Table 1. Segmentation results. Legend: (i) Severity of the pathology: no calcium(1)-multiple lesions(4); (ii) Image quality: bad(1)-excellent(4); (iii) Main branches detection: Yes/No; (iv) False positives: No/Ventricular wall - W (in parenthesis the starting point of the artefacts expressed as a proportion of the heart length)/Vein ; (v) Small branches tracking: poor(1)-excellent(4).

this part is less significant). These structures are part of the low ventricular wall which has a granulated texture which is interpreted by the algorithm as potential bifurcations of the artery. We propose a 2D-area filtering or a morphological 3D reconstruction in order to eliminate the problematic regions. This kind of 3D reconstruction has been used in[3] for similar purposes during the segmentation of the airway tree in CT images. Other kind of false candidates detected in few cases are the veins that cross very near the arteries and are selected as prolongations. Regarding the dependence on the parameters we find that if  $\mu_1 \uparrow$  or  $\lambda \downarrow$ , less significant details are extracted and false positives are obtained as well as all the small branches are tracked. If  $\mu_2 \uparrow$ , more potential vessel candidates are marked and consequently more details are captured. One of the main advantages in comparison to other methods is its independence from intensity variations during the acquisition procedure. Because of the local nature of the 2-dimensional slice analysis, the algorithm is able to follow the arteries in the presence of intensity changes between two slices. The algorithm also behaves in a robust way in presence of horizontal shifts between two slices (which is an important problem for the commercial stations) because of the associative field which permits to track the vessel even if it is misaligned. From a computational point of view the algorithm is quite efficient and the reconstruction is performed in a few seconds in a PentiumIV 3.2GHz, RAM-2GB.

## 4 Conclusions and perspectives

The proposed algorithm performs an efficient prior segmentation of the coronary tree from a one-click initialization. It doesn't lose any information, but in some cases gives false candidates in the more distal areas of the tree. It behaves in a robust way in the presence of intensity or displacement steps. A larger validation and optimiza-

tion of the parameters by including a learning process regarding different pathologies should be done. Concerning MACTSE, the most important restriction is the causality of the structures imposed to the model; which is biologically reasonable in our case but in other cases may not occur. MACSTE is currently being enhanced to follow non causal structures. We also may include a robustness module that permits to track the artery even when it disappears for some slices. Further developments will be devoted to assist in

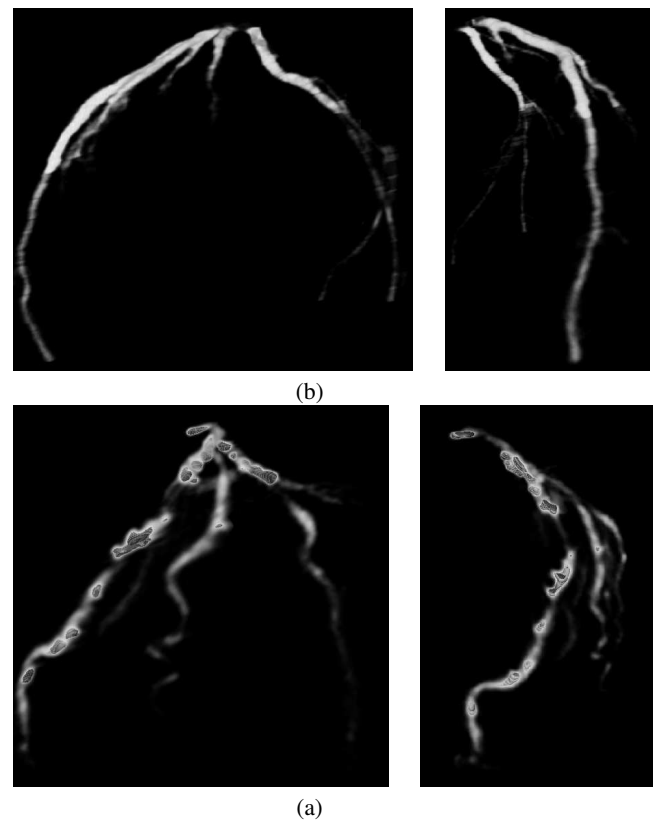


Figure 5. (a) Left coronary tree without lesions; (b) Left coronary tree with severe calcifications. The iso-surfaces superimposed to the rendering are at calcium-level intensity. Video renderings are available at [www.die.upm.es/im/videos/CT/](http://www.die.upm.es/im/videos/CT/).

the diagnosis of unhealthy arteries with quantitative data. Current state-of-the-art measurements of clinically significant parameters in order to obtain a quantitative estimation of stenoses or aneurysms is based on diameters and cross-sectional areas of vessels at different locations [4]. These measurements are strongly dependent on the estimation of the central axis which is a sensitive task specially in the presence of stenosis. As an alternative methodology, our future workplan is to develop directly a three dimensional segmentation based on the Hounsfield levels associated to each tissue and to measure volumetric parameters on this segmentation.

## Acknowledgements

This work was supported by the grant FPI-CAM(0362/2005) and projects PI041495 and PI052204, from the Spanish Health Ministry.

## References

- [1] Agin G. and Binford T. (1976) Computer description of curved objects. *IEEE Trans. on Comp.*, vol. C-25, pp. 439-449.
- [2] Angulo J., Nguyen-Khoa T., Massy F., Drüeke T. and Serra J. (2003) Morphological quantification of aortic calcification from low magnification images. *Image Analysis and Stereology*, Vol. 22, pp. 81-89
- [3] Bilgen D. (2000) Segmentation and analysis of the human airway tree from 3D x-ray CT images. Thesis. University of Iowa, Iowa City
- [4] Ferencik M, Lisauskas JB, Cury RC, Hoffmann U, Abbata S, Achenbach S, Karl WC, Brady TJ, Chan RC. (2006) Improved vessel morphology measurements in contrast-enhanced multi-detector computed tomography coronary angiography with non-linear post-processing. *Eur J Radiol*. Jan2006.
- [5] Field, D., Hayes, A., Hess, R. (1993). Contour integration by the human visual system: Evidence for a local association field. *Vision Res.*,33(2), 173- 193.
- [6] Florin C., Paragios N. and Williams J.,(2005) Particle Filters, a Quasi-Monte Carlo solution for segmentation of coronaries. *MICCAI05*, pages 246-253
- [7] Kiraly A.P.; Higgins W.E.; McLennan G.; Hoffman E.A.; Reinhardt J.M (2002) Three-Dimensional Human Airway Segmentation Methods for Clinical Virtual Bronchoscopy. *Academic Radiology*, Volume 9, Number 10, pp.1153-1168(16)
- [8] Kirbas, C. and Quek, F. (2004) A review of vessel extraction techniques and algorithms. *ACM Comput. Surv.* 36, 2, 81-121
- [9] Mueller D.; Maeder A. and O'Shea, P. (2005) Improved Direct Volume Visualization of the Coronary Arteries Using Fused Segmented Regions. *DICTA05* pages 110-118
- [10] Qian Y. and Eiho S.(2000) Morphological method for automatic. extraction of the coronary arteries. *Med Imaging.Tech*;18:231,238
- [11] Serra, J. (1982, 1988) *Image Analysis and Mathematical Morphology*. Vol I, II, Academic Press, London.
- [12] Vincent,L.(1993) Morphological grayscale reconstruction in image analysis: efficient algorithms and applications. *IEEE Transactions Image Processing*;2:176-201
- [13] Yang Y., Tannenbaum A., and Giddens D.(2004). Knowledge-Based 3D Segmentation and Reconstruction of Coronary Arteries Using CT Images. In *Proceedings of the 26th Annual International Conference of the IEEE EMBS*, pages 1664-1666
- [14] Zana, F. and Klein, J. (1997) Robust segmentation of vessels from retinal angiography. *IEEE International Conference on Digital Signal Processing*.Vol.2.1087-1090